Fe Segregation in Ti-10V-2Fe-3Al 30 Inch VAR Ingot β-Fleck Formation

J. A. Brooks, J. S. Krafcik, J. A. Schneider, and J. A. VanDenAvyle*
Sandia National Laboratories ICA, *NM

F. Spadafora
RMI Titanium Co.

Abstract

A 760 mm diameter VAR ingot of Ti-10-2-3 was melted under a wide range of conditions for validation of computer simulations predicting melt rate and melt pool shape, and to provide a better understanding of β-fleck formation. To study these effects the melt conditions were varied over large ranges. This report summarizes the metallurgical characterization of the ingot, and concentrates primarily on Fe segregation that can lead to the formation of β-fleck. Segregation of Fe could be associated with both low current magnetic stirring, and high current stirring used to mark pool boundaries. Segregation of Fe in regions along the ingot center was also observed. Mechanisms are proposed for the evolution of the Fe enrichment and its relationship to β-fleck formation observed in billet

Introduction

Ti-10Al-2Fe-3Al is a near β titanium alloy commonly used in aircraft components which is sometimes prone to the formation of β-fleck, single phase β regions in the heat treated microstructure (1,2). It is known that β-fleck is a melt related macrosegregation defect resulting primarily from an enrichment in Fe, although the mechanism by which the segregation occurs is not clearly understood. It is recognized that the tendency for β-fleck increases in material melted at high current and consequently with deep melt pools. A study had previously been conducted to characterize β-fleck in 200 mm diameter billet (3). Compositional analysis was conducted with an Omicron^{T} X-ray fluorescence instrument using line traces across regions of the sample that exhibited β–fleck. The β-fleck regions were found to be enriched in the β stabilizers, Fe and V by ~ 0.3-0.4 and 0.6-0.8 wt% respectively, and depleted in Ti and Al by ~1.0 and 0.3 wt% respectively. Although the nature of partitioning of the alloying elements was the same in all the β-fleck regions analyzed, the actual measured compositions did vary.

This report summarizes the metallurgical analysis of a Specialty Metals Processing Consortium (SMPC) industrial experiment conducted at RMI Titanium to study the formation of β-fleck in alloy Ti-10-2-3. Several goals of the experiment were to better define the relationship

between melt current and the occurrence of β-fleck and to increase our understanding of the mechanism by which the compositional variations occur which lead to β-fleck. An additional goal of the experiment was to provide pool shape data for bench marking VAR ingot computer simulations. However, the results of this simulation are not a part of this paper.

Experiment and Results

Melt conditions

A 760 mm (30 inch) diameter 2413 mm (95 inch) long ingot of Ti-10-2-3 was melted under a variety of conditions. It was thought that some of the melting conditions would yield billet material prone to β-fleck formation while other melting conditions would yield material that would be free of this defect. Although the specific melt schedule used in the experiment is proprietary, the general nature of the melting conditions will be discussed. The initial melting current was ramped to a mid-value where ~ 173 mm of ingot was melted (see Figure 2). The current was then ramped down to an intermediate level where approximately 818 mm of ingot was melted. At the end of this melting period a stirring current of 25 amps was used for 5 minutes to mark the pool boundary. The current was then ramped to the highest current level where approximately 363 mm of ingot was melted. Again high current stirring was used to mark the pool. The next section of ingot was melted at the same high current level except that low current magnetic stirring (5 amp) was used in which the direction of stirring was reversed every one minute. After this period the current was decreased to its lowest level for melting the remainder of the ingot. The first half of this final section was melted with low current stirring and the second half without.

After melting, the ingot was cut into four transverse sections each ~600 mm long. While maintaining orientation, these individual sections were cut longitudinally along the ingot centerline, and then cut to produce 25 mm thick slices from the faces of each of the four sections. These slices were again cut in half along their length. The half slices were then numbered with slice #1 at the bottom and slice #4 at the top, and represent the total ingot length. These slices were used for ingot metallurgical characterization. The other four full halves of ingot section were forged into 127 mm diameter billet, heat treated and characterized for β-fleck.

Characterization Techniques

Two x-ray fluorescence analyzers were used to map and quantify the macrosegregation. Sandia's x-ray fluorescence macroanalyzer (4) was used to generate overall elemental mappings of the sections of the ingot. The analysis was made with an excitation voltage setting of 10 keV on a Mo tube, using 1 cm and 3 mm diameter collimators. The ingot sections were further reduced in size and analyzed using an Omicron^{T} x-ray fluorescence analyzer for both elemental mappings and quantitative linescans. The Omicron analysis was made with an excitation voltage setting of 10 keV on a Mo tube with a 1 mm diameter collimator. Both machines were calibrated with Ti-10-2-3 standards placed at a set distance from the detector. Due to the large size grains of the ingot, some artifacts were observed in the Omicron analysis resulting from diffraction effects related to grain orientation with respect to the x-ray tube and detector.

Macrosegregation Characterization

The longitudinal ingot slices were compositionally mapped using Sandia's X-ray fluores-

cence macroanalyzer to determine the nature of macrosegregaton and establish correlations between macrosegregation and β-fleck formation. Compositional maps of Fe of two of the slices, slices #2 and #3, are shown in Figures 1(a) and (b). These maps were obtained with the macroanalyzer using a 1 cm beam and a 13x13 mm grid spacing. (The analysis for ingot slice #1, which was warped, is not included here.) A number of features are especially interesting in ingot slice #2. Bands both enriched and depleted in Fe which possibly outline the shape of the pool are readily apparent. These are present both in the bottom half and the very upper center of the slice. Regions higher in Fe are also seen as blotches near the ingot center.

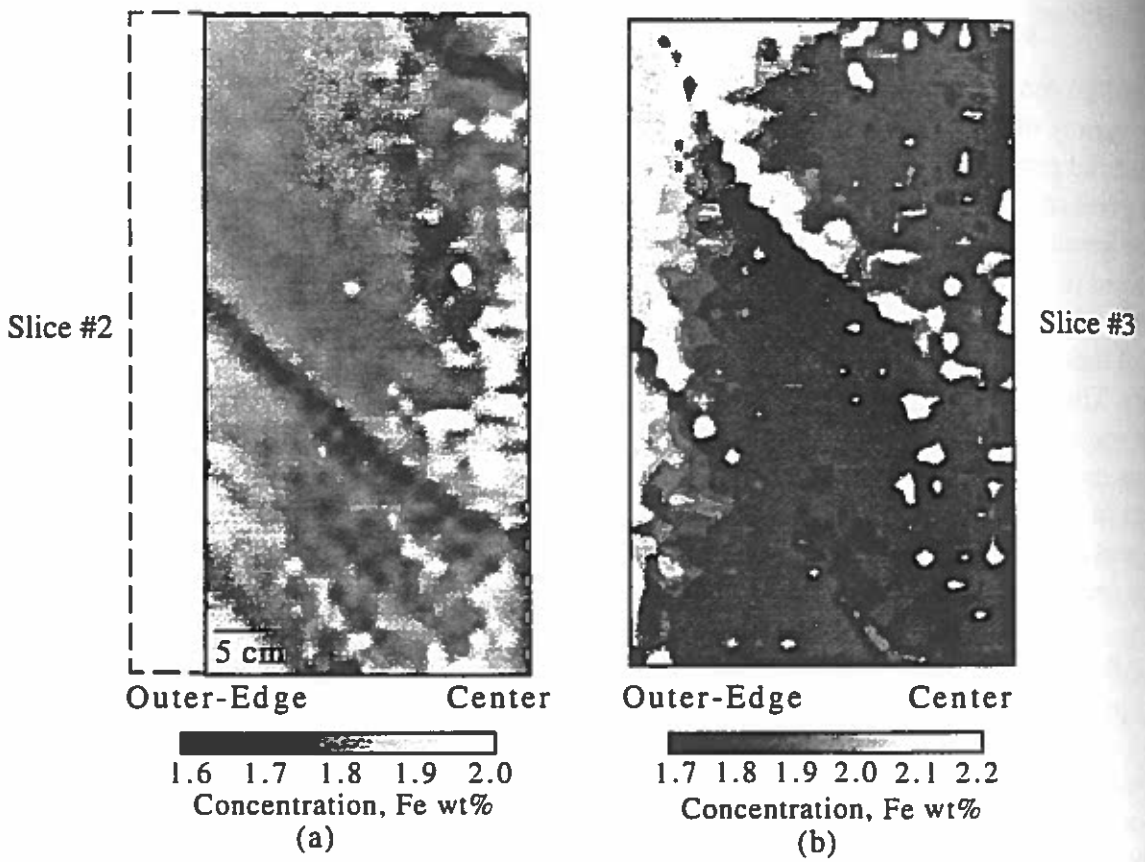

Figure 1. Compositional maps of Fe obtained using a 1 cm beam size and 13 mm grid spacing, (a) slice #2 and (b) slice #3.

The Fe lean band near the top center of slice #2, an apparent pool outline, can be seen to extend into slice #3, Figure 1 (b). A similar band, although in this case apparently high in Fe is clearly visible extending from the center of the ingot slice to the upper outer edge. Again some blotchy Fe rich regions are apparent near the center of the slice and possibly along the pool band.

The Fe compositional maps compiled together in Figure 2 represent the upper 75% of the ingot. The nature of the melting conditions is also noted adjacent to the compositional map. Also shown on the map are two regions, outlined by boxes, that were analyzed in more detail. Regions of β– fleck analysis are included in this figure but are discussed in a later section of the paper. It can be seen that many features of the compositional map can be correlated with changes in melt conditions.

Higher resolution compositional maps were made of a 10 cm high x 15 cm. wide (4 in. x 6 in.) rectangular section cut from the bottom center region of ingot slice #2, as noted in Figure 2. Figure 3(a) shows the macrostructure of the etched ingot section. The macrostructure is com-

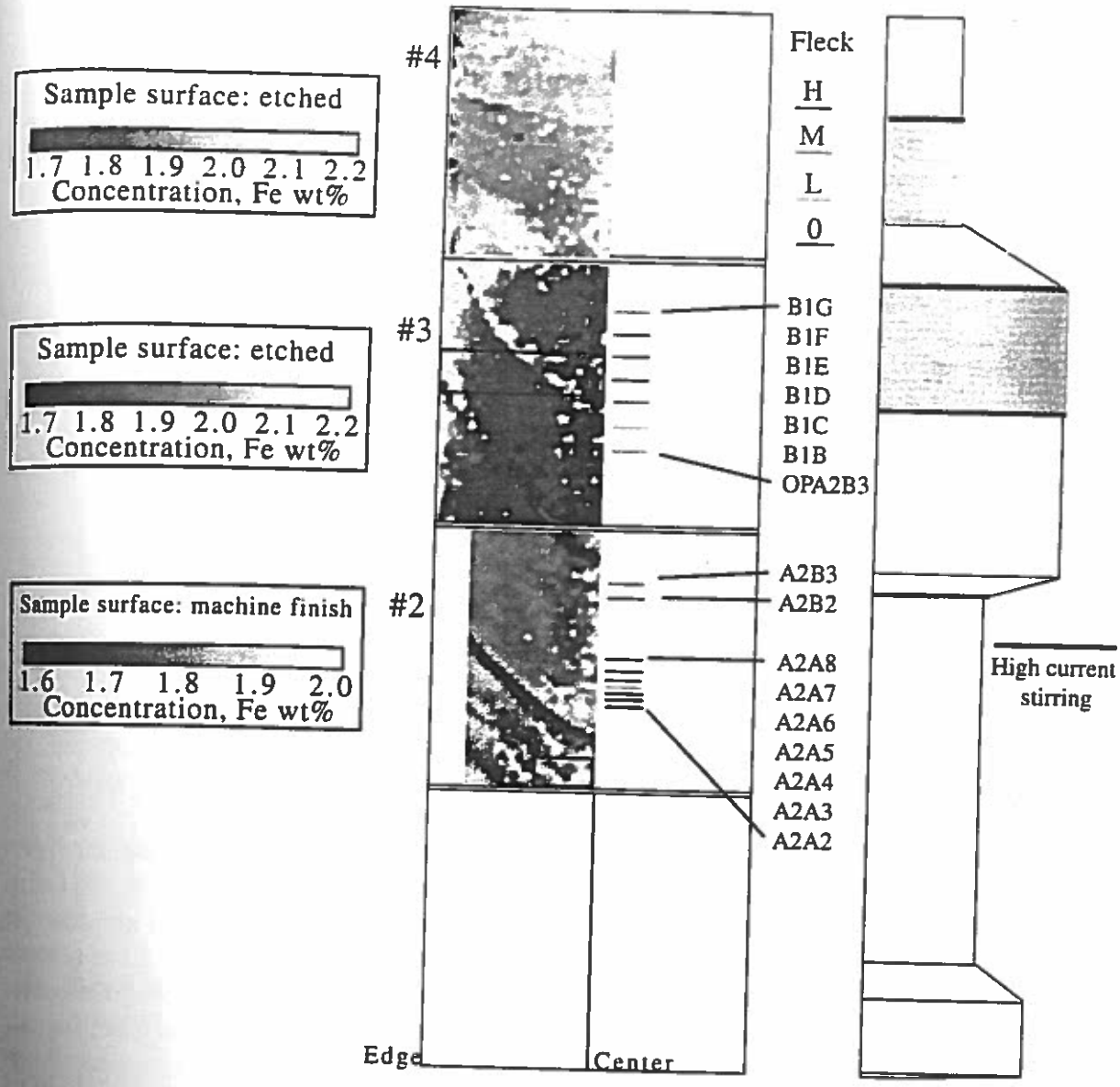

Figure 2. Composite of 3 XRF-Fe compositional maps comprising the top 75% of the ingot. A schematic of the melting conditions is shown to the right. Data was taken with a 1 cm beam and a 13x13 mm grid spacing. Note boxes outlined on slices #2 and 3 denote regions analyzed at a higher spatial resolution. Also shown are regions of β-fleck analysis taken from corresponding billet samples.

prised of large equiaxed grains typical of the total ingot except for a columnar structure that existed near the ingot bottom. Evidence of compositional "streaks" is apparent in the etched macrostructure. The corresponding Fe intensity map obtained using an Omicron X-ray fluorescence system with a 1 mm collimator is contained in Figure 3(b). It can be seen that the streaks are enriched in Fe. Although the spacing of the streaks is not uniform, the average vertical spacing is on the order of ~ 10 - 15 mm. It is also apparent that there is no correlation between the compositional streaks and the ingot grain structure. A compositional analysis was conducted across one of the streaked regions as indicated on both the X-ray map and etched macrostructure. The results for Ti, V, Al and Fe are also shown in Figure 3(c). It can be seen that the scan actually covered two streaks, one much more pronounced than the other. The region of the pronounced streak appears to be depleted in Ti and Al by ~2 wt% and 0.2 wt% respectively, and enriched in V and Fe by ~1

and 1.5 wt% respectively. The feature analyzed although rather narrow, ~6-7 mm, is still one of the widest streaks observed in the sample.

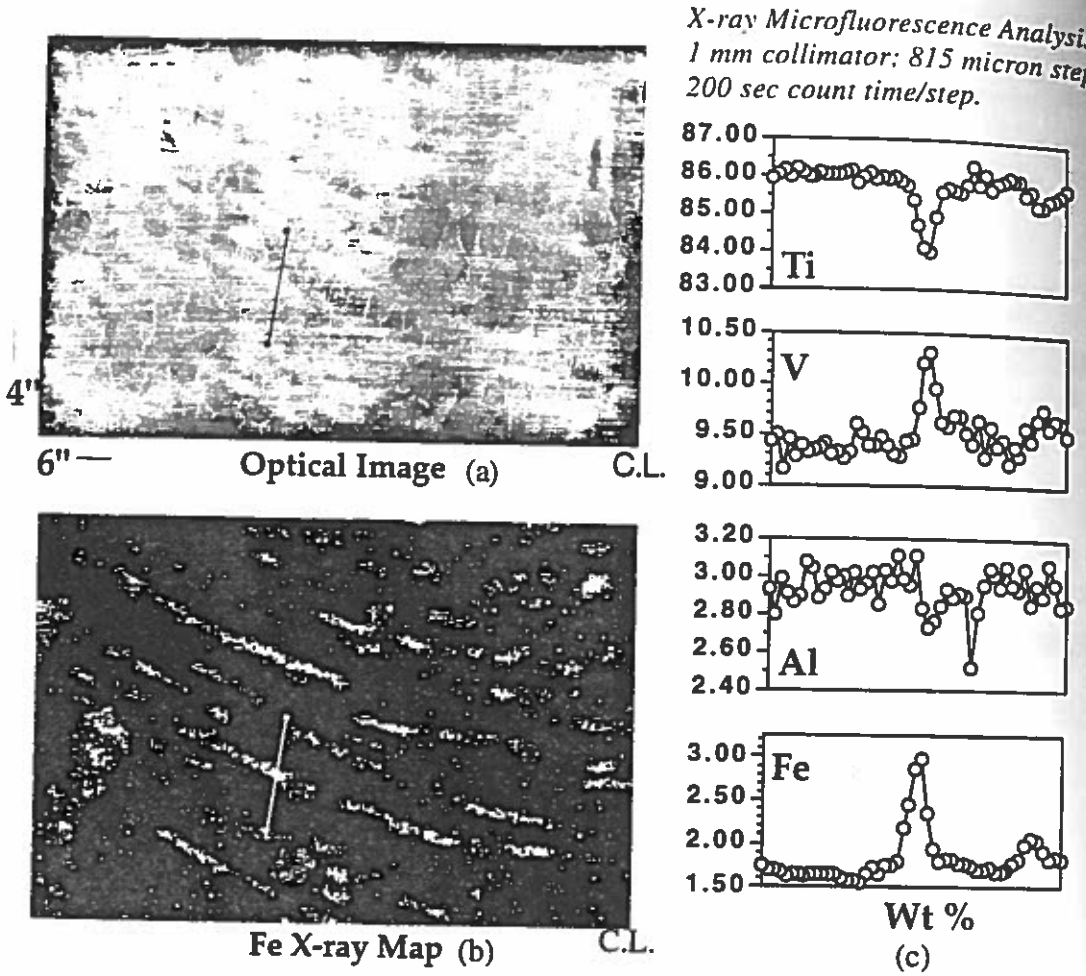

Figure 3. (a) Microstructure of bottom center region of ingot slice #2 in region noted in Figure 2. (b) Fe XRF intensity map obtained with the Omicron using a 1mm collimator. (c) Results from line scan (top to bottom) taken from region shown in (a) and (b).

After compositional mapping the sample was given a β-fleck heat treatment (800°C for 1 hr and water quenched) and electro-discharged machined (EDM) to remove a vertical slice 5 mm wide in the region where the line scan was taken in Figure 3. This and the adjacent section to the left (Figure 3) were then ground and etched in a dilute solution of nitric and hydrofluoric acid to reveal any β-fleck or Fe enriched features in the radial direction. Macrostructures of these samples are shown in Figure 4. The streaks can again be seen in the longitudinal section in Figure 4(a) as before although after heat treating and etching they are somewhat more pronounced. The strong correlation between the etched macrostructure and Fe content can be made by comparison with the X-ray map in Figure 3. The macrographs in Figure 4(b) show the nature of the streaks in the radial direction taken from the adjacent 5 mm slice. It can be seen that in this orientation the features appear as spots with the diameter similar to the width of the streaks in the longitudinal section. Also they are often associated with regions of grain boundary triple points. Thus the morphology of the Fe enriched regions appear to be pencil like in nature.

Higher resolution mapping was also conducted on ingot slice #3 in the region shown in Figure 2. The region encompasses a section from the center of the ingot to the outer edge with a height of ~96 mm. A composite map of Fe concentration comprised of 5 individual runs is shown

Figure 4. Macrostructure of sample shown in Figure 3 after sectioning and given a β-fleck heat treatment. (a) Longitudinal orientation to left of where line scan was taken in Figure 3. (b) Macrostructure of radial direction taken from slice adjacent to that shown in (a).

in the bottom of Figure 5. This data was obtained with the macroanalyzer using a 3 mm beam size and a 3 mm grid spacing which increased both the spatial as well as compositional resolution over that shown in Figure 1(b). Starting at the center of the ingot, one can see large blotchy regions enriched in Fe with measured values as high as 2.4%. A distinct compositional band runs at an angle of about 45° to the sample. To the right of the band (center section of the ingot) the average composition is higher than to the left of the band. This band very likely corresponds to the melt pool liquidus surface in a region where the melt current was changed and a high current stir was employed to mark the pool (see Figure 2). Also near the mid-radius region of the sample are smaller compositional bands nearly parallel to the distinct band discussed above. The vertical spacing of the smaller bands appear to be ~ 7 mm. It can be determined from Figure 2 that the finer banded region of the sample clearly solidified in a region in which low current magnetic stirring was used. After mapping, the region was EDM-ed from the ingot slice and sectioned into three pieces for photographing and further analysis. A montage of the three sections showing the equiaxed grain ingot macrostructure is also contained in Figure 5.

The center section (mid-radius) of the montage in Figure 5 was further mapped and analyzed with the Omicron using a 1 mm collimator. The Fe intensity map of this section, shown in Figure 6, exhibits the same banding as that shown in the macroanalyzer data in Figure 5. Other regions of Fe segregation are also evident in the intensity map. The measured variation in Fe in the stirring bands along the line noted on the X-ray map is shown graphically to be ~0.5 wt%. No other variation in alloying elements could be detected. After conducting the compositional analysis the sample was heat treated at 800°C for two hours, water quenched, and etched in an attempt to reveal any Fe-rich features. An image of the etched sample is shown to the left in Figure 6. The Fe enriched banding is very apparent as well as smaller horizontally oriented regions ~5-10 mm long. A subtle increase in intensity of the Fe maps clearly corresponded to these regions but they

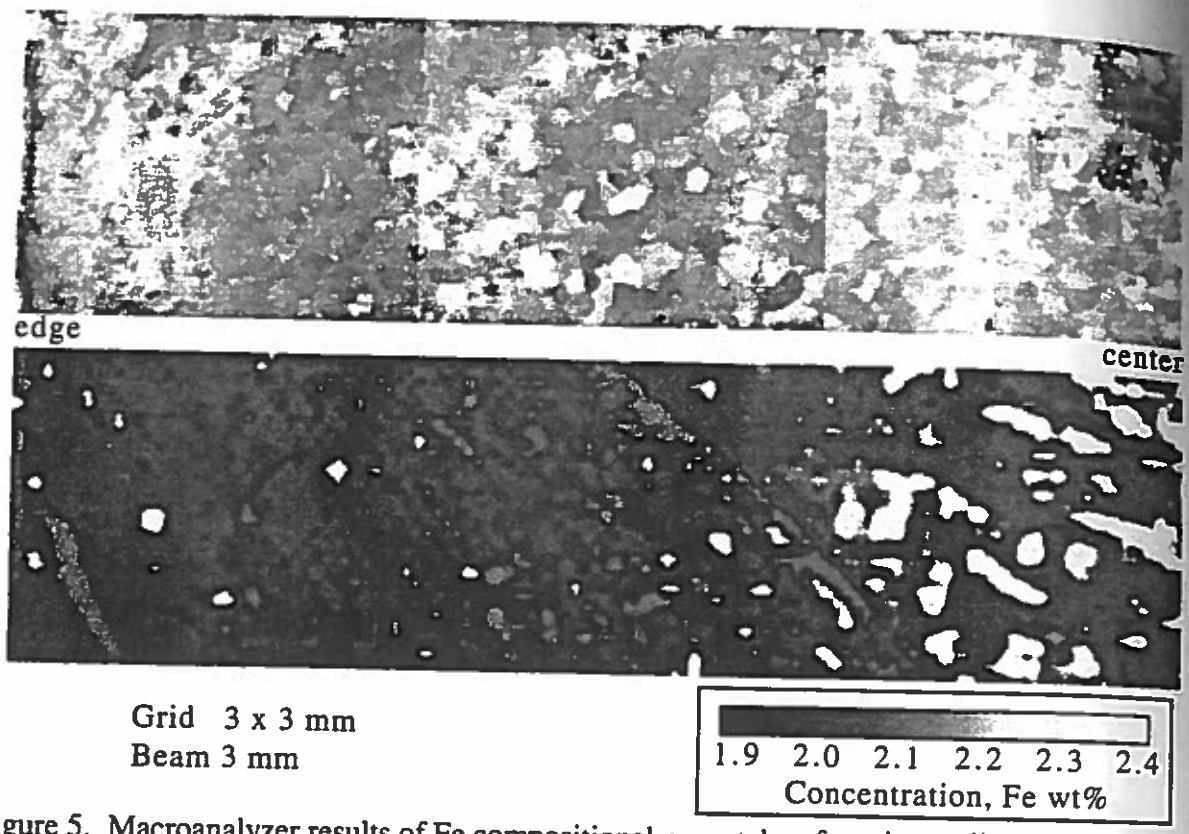

Figure 5. Macroanalyzer results of Fe compositional maps taken from ingot slice #3 in the region noted in Figure 2. Also shown above is the macrostructure in the corresponding region.

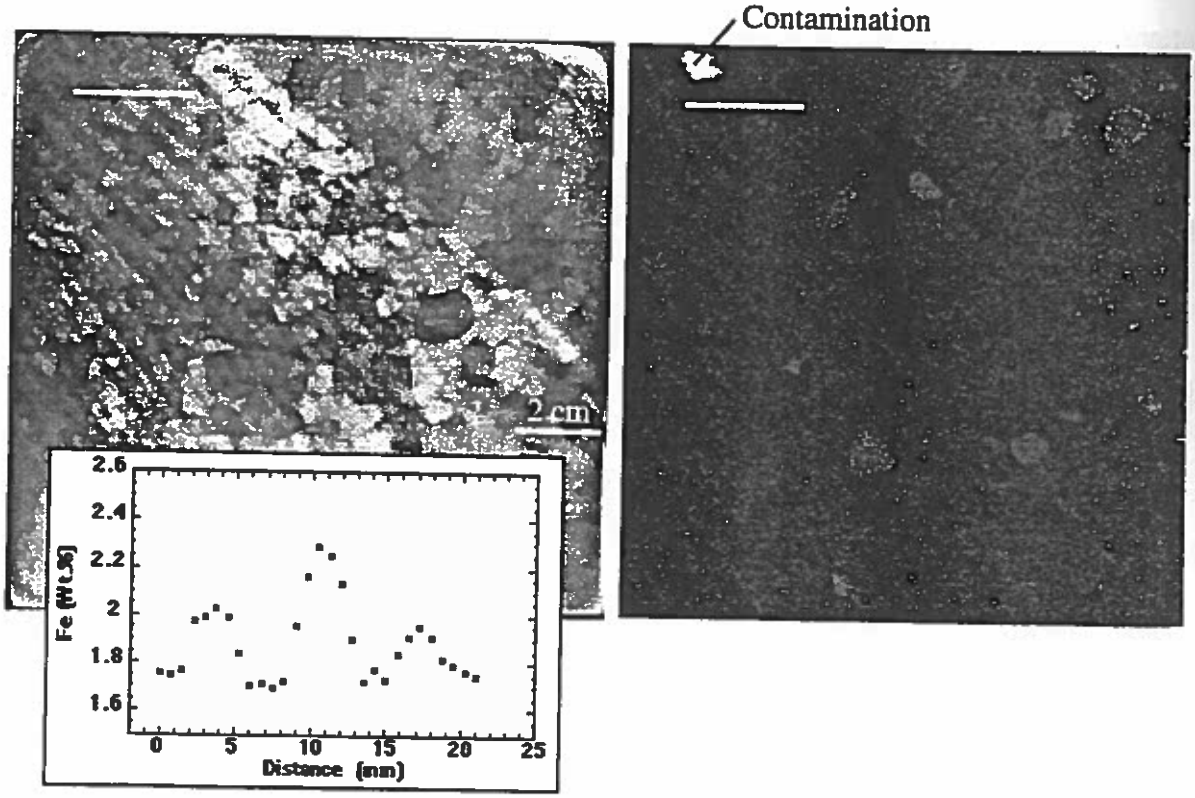

Figure 6. Omicron analysis of mid radius region of ingot shown in the montage in Figure 5. Fe intensity map to right obtained with a 1mm collimator. Note, well defined blocky regions in the Fe intensity map are artifacts due to diffraction from individual grains. To left is corresponding macrostructure and Fe analysis across stirring bands.

are lost in the transformation from color to gray scale for publication. However it is important to note that the high intensity blocky regions in the map are not apparent in the etched structure. By comparing the grain structure of the etched sample to the X-ray intensity maps, it was concluded that the larger well-defined blocky regions of high Fe intensity correspond to the grain structure, and are caused by a diffraction phenomenon. They are not due to any Fe enrichment. These regions should disappear and others appear if the sample were rotated to change diffraction conditions and then reanalyzed.

The adjacent section of sample at the ingot center, see Figure 5, was also analyzed with the Omicron using a 1 mm collimator. The Fe intensity map shown in Figure 7 again is similar to that obtained with the macroanalyzer shown in Figure 5. In this map many of the Fe enriched regions exhibit a linear character which is more apparent than in the macroanalyzer data. This is primarily due to the finer collimator (1 mm vs 3 mm) at which the data was obtained. Other better-defined blocky regions may be diffraction artifacts from individual grains as described above. A line trace

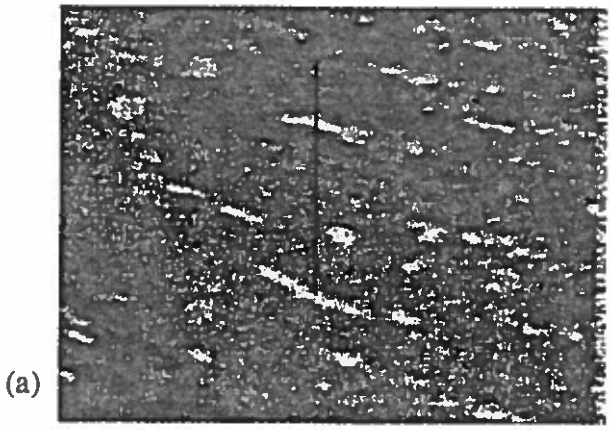

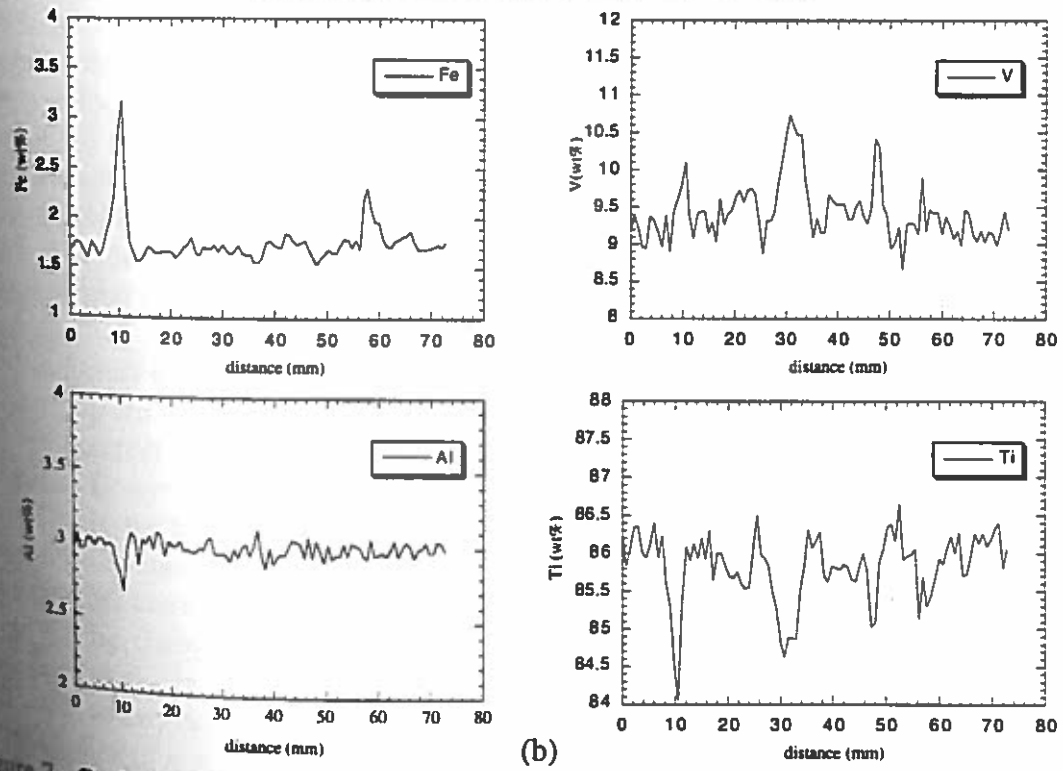

Figure 7. Omicron results from ingot center region of slice #3, section shown on the right in Figure 5. (a) Fe XRF intensity map (b) Compositional analysis taken from top to bottom along line shown in (a). Data was taken with a 1 mm collimator.

was conducted across several of the Fe enriched linear regions. These results are also shown in Figure 7. The data was obtained with a 1 mm collimator and a spacing of 0.75 mm. It can be seen that the Fe in the most intense regions has a measured concentration of ~1.5 wt% over the nominal measured concentration. In the region of highest Fe concentration it appears that there may be a corresponding enrichment of V and depletion of Al. There is a region near the center of the scan with a measured increase in V with the only measured accompanied change being that of Ti. This may correspond to a region in which some diffraction effects occurred, as discussed previously.

The above sample was also given the β-fleck heat treatment and etched to reveal the Fe rich features. A scanned image of this section is shown in Figure 8. The linear appearing Fe enriched regions of the compositional map directly correspond to the macroetched structure. A 6mm wide strip was further cut from this specimen and metallographically prepared as before to examine the radial direction normal to the longitudinal face of the sample. The orientation of this section is also shown schematically in Figure 8. It can be seen in the radial direction the Fe enriched regions again appear as round spots. The features thus appear to be of the same pencil shape morphology as was observed in the sample from slice #2. It was also found that many of the Fe enriched regions in the radial direction were near grain boundaries.

Selected regions of the forged 127 mm billet were sectioned, heat-treated at 800°C, polished, etched and examined for β-fleck. At least 16 sections were evaluated. The degree of β-fleck was characterized as: none, light, medium or heavy, and designated as 0, L, M, and H. In all the samples the regions of β-fleck correspond to the center portion of the ingot. The regions of the ingot from which the billet slices were taken and the corresponding β-fleck rating are shown along

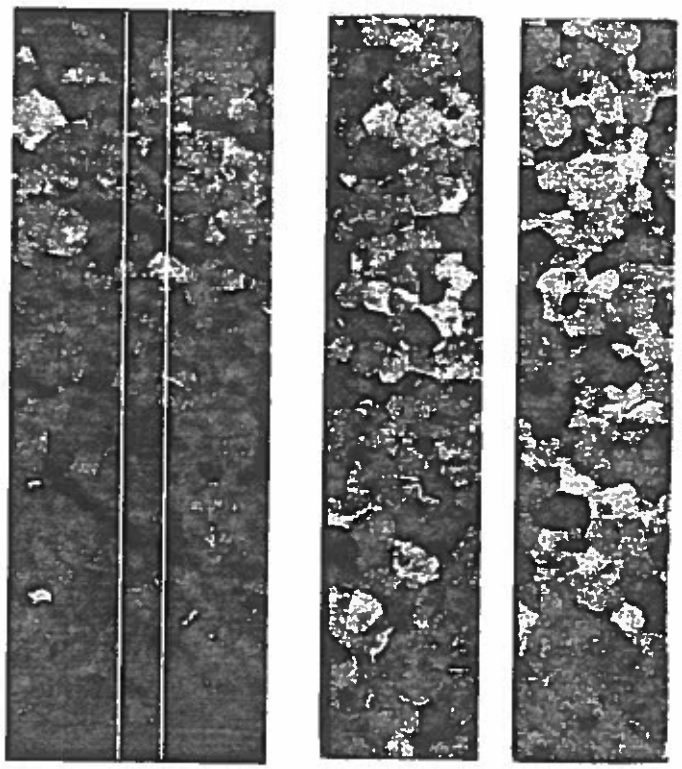

Figure 8. Etched ingot structure near center of ingot slice #3. Sample corresponts to the region where the line scan was taken in Figure 7. Macrostructures in (b) corresponds to the radial direction of the slice cut as noted in (a).

with the compositional map and melt schematic in Figure 2. An analysis was conducted on one of the samples with the heaviest rating of β-fleck using the Omicron with a 1 mm collimator. The measured increase in Fe content in the β-fleck was ~0.4 wt%, similar to that found in our earlier studies.

Discussion of Segregation Behavior

It can be seen from the X-ray fluorescence results that extensive macrosegregation exists in many regions of the ingot. It can also be seen that the segregation occurs on a number of length scales. However when viewing the data the beam size relative to the size of the features being analyzed must be kept in mind. For example the apparent degree of segregation in the center section of ingot slice #3 is considerably higher when measured with the Omicron using a 1 mm collimator than when measured with the macroanalyzer using a 3 mm collimator.

The compositional map of ingot slice #2, Figure 1(a) exhibits a considerable degree of macrosegregation even though it was obtained using a beam size of 1 cm. The majority of this slice was melted at the highest current with no magnetic stirring. High Fe concentrations exist in a number of regions along the ingot center. The Fe concentrations in these regions (higher than that measured with the 1 cm beam size) and may correspond to regions of β-fleck as discussed below. Several compositional bands are also apparent near the bottom of the slice. The position of the melt pool can be estimated from these compositional profiles and melt conditions shown in Figure 2. It can be seen that the most intense Fe depleted band corresponds to the position of the melt pool surface at the time of the first high current stir just prior to transitioning to a higher melt current. This band is depleted in Fe to a measured value as low as 1.6 to 1.7% Fe (using a 1 cm beam size) which then transitions to an enrichment in Fe to a measured value of ~2.1%. As noted above the compositional variation within the band may be higher than that measured with the rather large beam size. It is interesting to note that a Nb depleted band of similar appearance occurred during the high current stirring used for pool marking in Alloy 718 (5,6). The high current stirring may have swept some of the solute enriched interdendritic liquid from the outer region of the mushy zone leaving the Fe depleted band. This mechanism can result in an Fe enrichment of the pool in which subsequent solidification will occur at a higher Fe content similar to that shown in Figures 1(a) and 2. There is also evidence of somewhat wider compositional bands below the first stirring band shown in Figure 1(a). Since these bands occur in a region of constant current melting, the mechanism by which they form is not obvious

In further examining the Fe X-ray maps of the total ingot, Figure 2, at least four regions of pool marking are evident. These four regions correspond to the position of the pool boundary when high current stirring was employed and can be used to compare with code predictions of pool shape. However, it is interesting to note that the compositional nature of the bands is not the same. That is, the bottom two distinct bands are first depleted in Fe, while the upper two bands appear to be Fe enriched. For the top two bands a termination of magnetic stirring directly followed the high current stir. In addition to sweeping of interdendritic liquid resulting from high current stirring, changes in thermal gradients resulting from perturbations in melt or solidification conditions can also result in solute lean or enriched bands as modeled by Flemings and Mehrabian (7,8). Stirring may have reduced the thermal gradients ahead of the solidification front. Likewise the termination of stirring may have increased the thermal gradients. In the first case one would expect, from a Mehrabian-Flemings type analysis, a solute depleted band while in the second case, an increase in thermal gradient in the liquid, one may expect the formation of a solute dump or enriched band. It is interesting to note that this is consistent with the solute content of the three

pool marking bands in the upper region of the ingot. However, it has been suggested that this type of segregation behavior exists in columnar dendritic solidification structures but not in regions of equiaxed grains as observed here (9). It can be seen that other changes were being made in the melting conditions at the middle two bands which also affect the solidification conditions. The interactions of sweeping of interdendritic liquid during high current stirring and changes in thermal gradients and growth rates are very complex and can best be studied using ingot solidification codes which model mushy zone behavior. The point to be made here is that abrupt changes in melting conditions and magnetic stirring can result in significant compositional differences that in some cases may lead to the formation of β-fleck in billet product.

There are also other regions of large scale macrosegregation in the ingot, Figure 2. The outer radius of the ingot slice #3 is enriched in Fe, especially the top region. It can also be seen in the upper region of the composite compositional maps in Figure 2 that the pool depth became considerably shallower when the melt current was reduced over a 50 minute interval from the highest to the lowest values used in the experiment. During this time the center region of the solidifying ingot also became depleted in Fe and the outer region of the ingot enriched in Fe. These regions correspond to the top center section of ingot slice #3 and the outer lower region of slice #4. During melting at the lowest current with magnetic stirring, the center region of the ingot appears to have become enriched in Fe. This large-scale macrosegregation behavior results from changes in the complex fluid flows as melt conditions vary.

Beta Fleck

As noted above, one of the primary goals of this experiment was to determine the mechanism of β-fleck formation. It is known that β-fleck is associated with the enrichment of Fe and V β-stabilizers and that these elements segregate to the liquid during solidification (k<1). The severity of β-fleck in the regions of billet analyzed is shown with the compositional map and melt schematic in Figure 2. It can be seen that data on β-fleck analysis of the billet is available in only very select regions.

It must be emphasized that the melt conditions for this ingot are far from those commonly used in production since the goal of the experiment was to validate the VAR melting code as well as to study the formation of β–fleck. Thus the large compositional changes due to high current stirring and the large changes in melt current are not common, although the occurrence of β-fleck is not unusual. Therefore only the features that may be more representative of production ingots will be discussed with respect to β-fleck.

There are several regions of special interest that were studied in detail and will be discussed further. Variations in composition resulted from low current magnetic stirring as indicated by the banding to the outside of the large stirring band shown in Figures 5 and 6. This section of ingot exhibiting the fine scale banding was melted at the highest current and with the use of low current magnetic stirring. The average spacing of the bands, ~7 mm, corresponds to the amount of melting that occurs in one complete current cycle (2 minutes). This is strong evidence that the segregation effect is a direct result of the low current stirring and that the stirring current affects the solidification conditions and concentrations of solute at the solidification front. The variation in Fe in the bands was ~ 0.5 wt%, on the order of that observed in β-fleck in billet.

The effect of homogenization on compositional variations can be estimated knowing the morphology of the macrosegregation region and the diffusion coefficients as shown by Shamblen

in Ti-17 (10). The expression shown in Figure 9 (11) is appropriate for determining the homogenization behavior of the low current stirring bands shown in Figures 5 and 6. It can be seen that the degree of homogenization is dependent upon both the diffusivity and the band spacing. To reduce the variation in Fe by 50%, from 0.5 wt% to 0.25 wt%, a homogenization time of ~ 3 hrs would be required at a homogenization temperature of 1400°C, ~200°C below the solidus temperature (This is assuming the diffusivity of Fe as $D_0 = 0.6\ cm^2/sec$ and Q=45kcal/mole (12)). The same degree of homogenization with a 6 to 1 reduction of the 760 mm ingot to 127 mm billet, (band spacing reduced form 7 mm to 1.2 mm) and a solution treatment of 1200°C would take only ~1/2 hrs. However, if one uses a diffusivity obtained by Shamblin (10) for Cr in Ti-17, ($D_0 = .07\ cm^2/sec$ and Q=46.5 kcal/mole) which may be similar to that of Fe in Ti-10-2-3, the times calculated for the same degree of homogenization increase to ~40 and 8 hrs respectively. Although this demonstrates the importance of knowing diffusivities, it is likely that during ingot homogenization and breakdown the segregation due to low current stirring may decrease significantly. It is not likely a source of β-fleck in forged billet since Fe composition in the stirring bands without homogenization is similar to that of β-fleck in processed material.

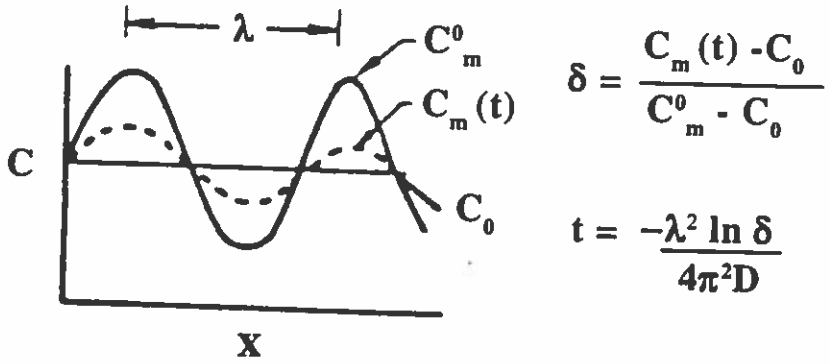

Figure 9. Analysis used to predict homogenization of low current induced banding such as that shown in Figures 5 and 6, ref. 8.

However, there are several other regions of the ingot in which larger compositional variations in Fe were observed. These are near the bottom center of ingot slice #2, Figure 3, and at the centerline region of ingot slice #3, Figures 5 and 7. In both of these regions the Fe enrichment was in the form of channels which appeared to be fairly closely aligned with the liquidus interface. The measured Fe concentrations in these regions was as high as ~1.5wt% above nominal, similar to values reported by other investigators (13). There was also an accompanied measured enrichment of ~1wt% V with only a slight depletion of Al in the same regions. It was further found that the Fe enriched regions were generally confined to grain boundary regions and triple points. With the high concentration of β stabilizers, Fe, and the rather large diffusion distances, homogenization will be more difficult than that of the stirring bands. Thus it appears that these are regions of ingot that can result in β–fleck in billet. During ingot homogenization and breakdown the concentration of Fe and V will be reduced but maybe only to values commonly observed in β-fleck. That would be concentrations of ~ 3.2 to 3.5 wt% Fe being reduced to values of ~2.4 wt%.

It has been suggested that β-fleck formation in Ti 10-2-3 occurs by the filtering of solute rich liquid through the rather open dendritic network in a direction approximately parallel to the liquidus line (14). The higher density of the interdendritic liquid is responsible for the downward flow but no dissolution occurs. However it is not clear why such long channels would form by such a mechanism. It is clear from this study that channels only a few millimeters in diameter can extend in a fairly linear manner in some cases over distances of many grain diameters.

It is proposed here that the macrosegregation of Fe and V in the long pencil like morphology may form by a similar mechanism as channel defects or freckles proposed for a Ni-based superalloy (15,16). This mechanism is shown schematically in Figure 10 for a columnar dendritic solidifying structure. These defects can appear fairly linear in nature in a longitudinal cross section with an orientation close to that of the pool liquidus interface. A requirement for this type of channel to form is that the density of the interdendritic liquid increases during the solidification process. This criteria is clearly met in Ti-10-2-3 with the interdendritic segregation of Fe and V (k, the partitioning coefficients <1). The other requirement is that the freckle grows into an increasing temperature field for a dissolution mechanism to occur and the channel to propagate. It was apparent in a heat of Alloy 718 that the freckles propagated by this dissolution mechanism in a downward direction yet into an increasing temperature field. Extensive evidence of dissolution and dendrite fragmentation was also observed in the freckle channel.

This schematic should be somewhat modified for an equiaxed grain structure. In this case as the grains start to impinge, higher density interdendritic liquid can flow in a downward direction. The channels that can most easily propagate will be those in regions of the grain boundaries of several intersecting grains. However, to form a channel like freckle, by this dissolution mechanism flow must continue into an increasing temperature field. With an equiaxed structure the potential paths are more limited than in a columnar dendritic structure. If the propagating channel intersects the central region of a grain, flow will have a tendency to change to either a more upward or downward direction. A more upward direction would reduce the gravitational driving force and a more downward direction would reduce the temperature field. Either of these changes could result in termination of channel formation. This could explain the rather short channel length observed compared to that common in other alloys. Most of the channel type freckle defects appeared to be only a few grain diameters in length although some extended 8-10 grain diameters in the plane of sectioning.

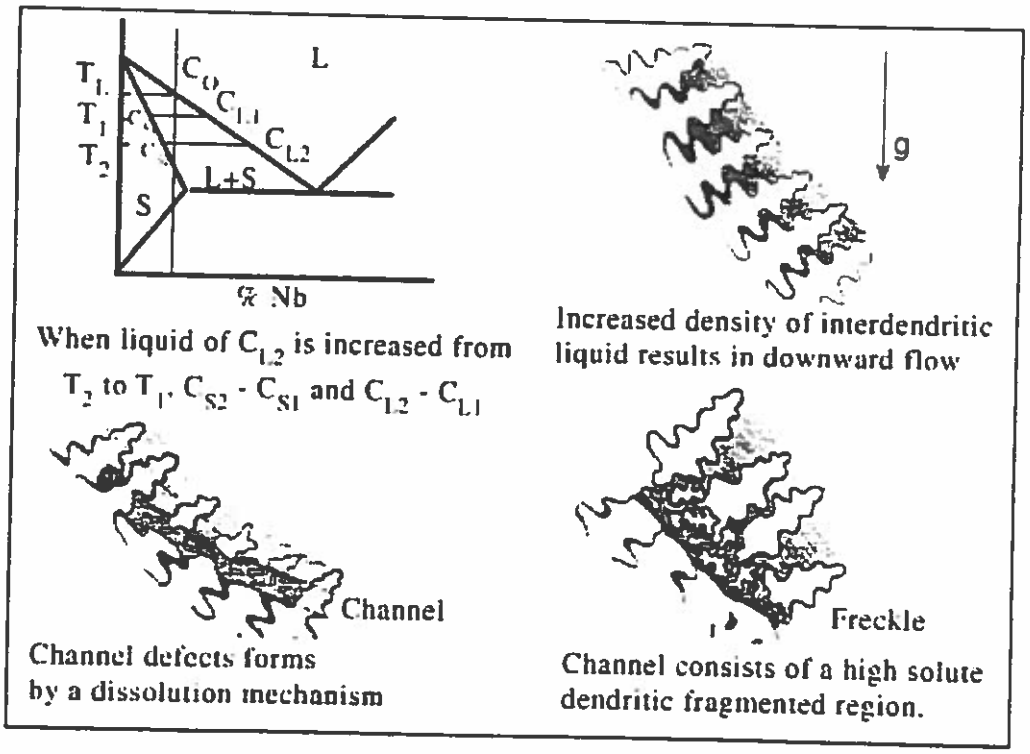

Figure 10. Schematic of formation mechanism of channel type freckle forming in a columnar dendritic solidifying structure.

For a channel type defect to form, as suggested here, the channel must propagate in an increasing temperature field. For this to occur the slope of the channel will be less than that of the isotherms at its front. The band in the bottom left corner of the Figure 7 corresponds to the position of the solidifying interface at the time of stirring. It appears that the slope of the high Fe rich channels is less than that of the interface. If the pool interface maintains the same orientation as solidification progresses, then it appears that these Fe rich regions could be channels that are growing into a higher temperature region. However, no change in structure was associated with the channel appearing regions. This may be a result of homogenization occurring on the microsegregation scale during solidification and cooling making detection of the dendrite structure difficult. It also should be noted that the filtering of high solute content liquid along an isotherm of the mushy zone could have a tendency to have a similar orientation with respect to the pool isotherms, that is laying at a lesser slope.

There are also smaller regions of higher Fe concentration visible in the etched heat treated ingot (dark etching features apparent near the center of the sample) and the Fe intensity map shown in Figures 3,6, and 8. These are smaller regions than the long channel type features and are similar in size to that of the grains. These may have occurred from the segregation of intergranular liquid, or small segregate pools, similar to freckle formation in Alloy 625 ESR material (17). In some cases shorter channels with some dissolution may also occur.

An analysis can also be conducted to estimate the degree of homogenization that may occur as a result of ingot homogenization and breakdown of the Fe enriched channels. In this case the appropriate analytical solution would be that of an infinitely long rod of one composition in a matrix of another composition. The solution in graphical form is shown in Figure 11 for a rod of radius a and different values of Dt/a^2. Using a radius of a channel of 3mm and the Fe diffusivities used above, a reduction of Fe from 3.5% to 2.6% in the 2% Fe alloy (Dt/a^2=.5) would require a ~16hrs homogenization at 1400°C. However, if the lower diffusivity is used, that of Fe in Ti-17 as discusses above, the diffusion time increases to ~212 hrs. This is degree of homogenization that would result in Fe concentrations commonly observed in β-fleck of forged billet.

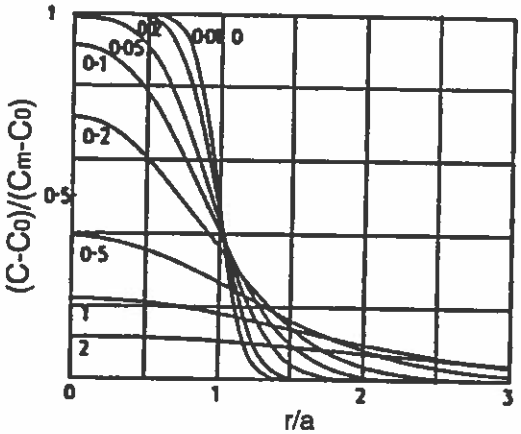

Figure 11. Concentrations resulting from an infinite long region of radius a of concentration C_m embedded in matrix of another concentration, C_0 , for different values of the Dt/a^2, from ref 18.

Summary

It was found in this experimentally melted ingot of Ti-10-2-3 that changes in melt param-

eters resulted in large compositional variations occurring on several different length scales. The use of the X-ray fluorescence techniques was very useful in determining the nature of the macrosegregation patterns. Large changes in melt conditions resulted in significant macrosegregation of alloying elements. It was found in etched billet that β-fleck was confined primarily to the center of the billet as is commonly observed, and was associated with an enrichment of ~0.4wt% Fe and 1 wt% V. Fe segregation was associated with low cycle magnetic stirring, but it was concluded that the concentrations and spacing were such they would likely be homogenized during ingot breakdown. Regions with high measured concentrations of Fe exhibiting a somewhat linear morphology were observed in regions along the ingot center. It is proposed that these features with measured Fe concentrations as high 3.5 wt% are the source of β-fleck observed in billet. It was further proposed that the features form as channel type segregates or freckles. Analysis were conducted to determine the effect of homogenization schedule on reducing β-fleck, but the results are highly dependent upon diffusion rates.

Acknowledgments

The authors would like to thank the large number of workers at RMI and Sandia who conducted the melt experiment. Also help with metallographic preparation of samples by Andy Gardia of Sandia in Livermore, CA. is greatly appreciated This work was supported by the U. S. Department of Energy and the Specialty Metals Processing Consortium.

References

1. C. C. Chen and R. R. Boyer: J. of Metals, 7-79, pp. 33-39.
2. T. W. Duerig, G. T. Terlinde and J. C. Williams: Phase Transformations and Tensile Properties of Ti-10V-2Fe-3Al, Metall. Trans. A, vol. 11A, 12-1980, pp 1987-98.
3. D. Boehme, J. Brooks, and J. Krafcik: "Analysis of Ti-10-2-3 Beta Fleck, SMPC report, 6-96.
4. J. S. Krafcik and J. A. Brooks: "Compositional Mapping of Large Samples Using X-Ray Fluorescence", in conf. proc. Developments in Materials Characterization Technologies, July 95, Albuquerque, NM, Ed G. Vander Voort and J, Friel, pub Inter. Metallo.Soc. and ASM p.111-118.
5. J. Brooks, J. Krafcik, R. Williamson and C. Adasczik: "Metallurgical Analysis of Teledyne Allvac 718 VAR Ingots", SMPC report, December 1994.
6. J. Brooks, J. Krafcik and D. Boehme: "On White Spot Formation in the Nb Strengthened Superalloys Incomel 706 and 718", SMPC report June 94.
7. M. C. Flemings, R. Mehrabian and G. E. Nereo, Trans. TMS-AIME, 1968, vol.242, pp. 41-49.
8. R. Mehrabian, B. H. Kear, and M. C. Flemings: Metall. Trans, 1970, p. 1209.
9. A. Mitchell and D. Tripp: "Solidification and Segregation in Titanium Alloys, Int'l Conf. on Titaniun Products and Applications, Vol.II, 1986, San Francisco, CA, pp1011-1019.
10. C. Shamblin: Metall. Trans. B, Vol. 28B, 1997, pp. 899-903.
11. M. Cohen, B. H. Kear, and R. Mehrabian: Rapid Solidification Processing- Principles and Technologies II, pub.Claitor's, 1980, pp. 1-23.
12. Smithells and Brandes: Metals Reference Book 5th ed. p.914.
13. Y. G. Zhou, J. L. Tang, H. Q. Yu and W. D. Zeng: "Titanium 92" eds. F. H. Froes and I. L. Caplin, publ. TMS-AIME Warrendale PA, 1992, 1, pp. 513-521.
14. P. Auburtin, C. Edie, B. Foster, I. Mackenzie, A. Mitchell and A. Schmalz: Proceedings 1997 International Symposium on Liquid Metal Processing and Casting, Sante Fe NM, pp.60-77.
15. J. Brooks, J. Krafcik, and F. Zanner: Metallurgical Analysis of a 520 mm Diameter Inconel,718 VAR Ingot, SMPC report 8-93.
16. J. Van Den Avyle, J. Brooks and A..Powell: "Reducing Defects in Remelting Processes for High-Performance Alloys", JOM, 50 (3) 1998, pp.22-25.
17. J. Brooks, J. Krafcik, J. Van Den Avyle, and R. Schunk: Inco Alloy 625 ESR Freckle Experiments, SMPC report August 1997.
18. H. S. Carslaw and J. C. Yager: "Conduction of Heat in Solids", Second ed. Clarendon Press, Oxford, 1986.